Control of Wind Energy Conversion System under Typhoon Landed Conditions

Dr.D.Chandra Sekhar, Veerala Geetha

Abstract— This paper presents control approach for the PMSG based WECS under a wide range of wind speeds. Generally most of the wind turbines are turned-off & disconnected from the power grid, in case wind velocity is over 25m/s. This project uses pitch angle controller and rotational speed control systems that the PMSG based WECS can generate power if the speed are above 25m/s. The proposed method reduces mechanical stresses of the wind turbine by preferential reducing of the rotational speed rather than the mechanical torque during strong wind conditions. The chance of turning off is reduced compared to the conventional control system because the PMSG based WECS can temporarily tolerate the wind speed up to 35m/s.

Index Terms— *Grid Side Converter (GSC), Insulated Gate Bipolar Transistors (IGBT), Machine-Side Converter (MSC),* MPPT control , PI controller , *PMSG based WECS, Variable-Speed Wind Turbine (VSWT).*

1 Introduction

THIS document is a Consumption of fossil fuels for generating electric power causes environmental pollutions and possible global warming. Alternatively, electric power generation by the nuclear power plants is risky due to the unreliable behavior of the plant and the possible challenges of nuclear waste dumping. Therefore, electric power generation using renewable energies are gaining huge momentum around the world. Common sources of renewable energies are wind power, solar energy, hydropower, bio-fuel and so on. Among them, WECS has the largest market share and is expected to maintain rapid growth in the coming years.

Usually, WECS uses two types of wind turbines: Variable-Speed Wind Turbine (VSWT) and Fixed Speed Wind Turbine (FSWT). The VSWTs have many advantages such as Maximum Power Point Tracking (MPPT) during operation, better performance and control of the power output. In recent years, the use of VSWTs with the PMSGs have been increased because of their higher efficiency, simpler structure and easy maintenance compared to the other generators.

Generally, the AC-DC-AC power conversion system is utilized as the basic topology for the PMSG based WECS. This kind of topology does not require synchronizing the rotational speed with the grid frequency. Also, the gearbox can be omitted for the directly driven operation of the PMSG. Therefore, a PMSG based WECS with AC-DC-AC conversion circuit is a subject of research in this paper, specially its operation in the strong wind conditions. Mechanical stress due to strong wind conditions is one of the operational challenges for WECS. Japan is a typhoon prone country, more specifically Okinawa prefecture of Japan faces one average 11 typhoons every year. When the wind speed exceeds 25 m/s, most wind turbines stop the power generation and are shut down. It reduces energy utilization efficiency of the WECS. In addition, shutting down of the large wind turbine or wind farm causes severe frequency fluctuations which may lead to the power system instability and a cascaded failure.

In an adaptive control strategy is proposed for reducing extreme loads and fatigues of the wind turbine when operated under high wind speeds. However, as the wind turbine is operated at the rated speed in the high wind conditions, it could be a matter of safety concern. As the cause of main mechanical stress is centrifugal force rather than the wind pressure, unexpected rise in the rotational speed warrants a serious caution. An Artificial Neural Network (ANN) based pitch angle control is developed in. It can operate in the wide range of wind speed, however; mechanical stress at the high wind speeds is not considered in the development of the pitch angle controller.

Considering the research gaps of and, a novel control strategy for the PMSG based WECS is presented in this paper. The novelty lies within the consideration that the proposed control strategy reduced mechanical loads the wind turbine by a preferential reduction of the rotation speeds and not by reducing the mechanical torque during strong wind conditions. In the proposed method, the PMSG based WECS can temporarily tolerate wind speed up to 35 m/s. As a result, the WECS can generate power during strong wind conditions which is important for a typhoon prone area like Okinawa. Performance of the proposed control system is verified via numerical simulation results obtained in the MATLAB/Sim Power Systems environment.

2 Wind Energy Conversion Systems

2.1 Wind Energy Conversion System

A generic single line diagram of a PMSG based WECS is shown in fig (2.1) .Wind energy is converted to variable frequency electric power by the PMSG. This power is supplied to the grid after converting it to a fixed frequency electric power via the AC-DC-AC conversion systems which comprises of a Machine-Side Converter (MSC) and a Grid Side Converter (GSC) connected by a DC-link capacitor. The GSC controls the rotational speed, as well as the output power of the PMSG. The system after the DC link is modeled as a voltage source

because the system is the same as a conventional system.

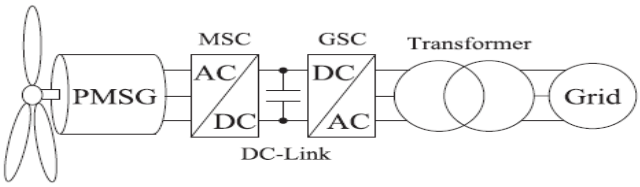

Fig.2.1. Line Diagram of a PMSG based WECS

2.2 Wind Turbine Model

Fig.2.2 shows the wind turbine and the PMSG models. The wind turbine converts wind energy to mechanical power *Pw*. The mechanical power *Pw* extracted from the wind is expressed as:

$$\mathrm{Pw} = \frac{1}{2} C\mathrm{p}(\lambda,\beta)\rho\pi R^2 \mathrm{V_w^3} \qquad (1)$$

Where Cp is the power coefficient of the wind turbine, k = ymR/Vw is the tip speed ratio, ym is the wind turbine mechanical rotational speed, b is the pitch angle, q is the air density, R is the radius of the wind turbine blades and Vw is the wind velocity.

The wind turbine input mechanical torque *Tm* is given by:

$$\mathrm{Pw} = \frac{1}{2} C\mathrm{p}(\lambda,\beta)\rho\pi R^2 \mathrm{V_w^3} \qquad (1)$$

and the power coefficient of wind turbine *Cp* is given by the following equations

$$\mathrm{Cp} = 0.22\left(\frac{116}{\lambda \mathrm{i}} - 0.4\beta - 5\right)\exp^{\frac{-12.5}{\lambda \mathrm{i}}} \qquad (3)$$

$$\lambda \mathrm{i} = \frac{1}{\frac{1}{\lambda + 0.08\beta} - \frac{0.035}{\beta^3 + 1}} \qquad (4)$$

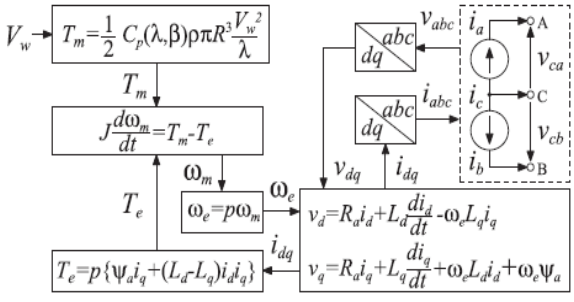

Fig.2.2. Block Diagram of Wind Turbine Model

2.3 PMSG Model

The mathematical model of a PMSG is the same as the Permanent Magnet Synchronous Motor (PMSM). PMSG is modeled in the synchronous d-q frames by the following voltage and electrical torque equations;

$$v_d = R_a i_d + L_d\frac{di_d}{dt} - \omega_e L_q i_q \qquad (5)$$

$$v_q = \omega_e L_d i_d + R_a i_q + L_q\frac{di_q}{dt} + \omega_e K \qquad (6)$$

$$T_e = p\{Ki_q + (L_d - L_q)i_d i_q\} \qquad (7)$$

where *vd* is the *d*-axis voltage and *vq* is the *q*-axis voltage, *id* is the *d*-axis current and *iq* is the *q*-axis current, *Ra* is the stator resistance, *Ld* is the *d*-axis inductance and *Lq* is the *q*-axis inductance, *ye* is the electrical rotational speed, *K* is the magnetic flux, and *p* is the number of pole pairs. The motion equation is expressed as the following;

$$J\frac{d\omega_e}{dt} = T_m - T_e \qquad (8)$$

where *J* is the inertia.

2.4 Configuration of The Control Systems

The MSC is comprised of six Insulated Gate Bipolar Transistors (IGBT) which are switched ON/OFF by using the triangular-wave PWM method. The control is based on the measurements of wind speed, generator voltages, currents, and rotational speed. Although, wind speed measurement in WECS control is not recommended. However, appropriate output power is defined based on the measured wind speed in this research. This is because determination of the operating area is important to ensure safety in the strong wind condition. Naturally, typical wind speed estimation can be also applied to the system as in. An anemometer is used for simplicity in this paper. The details of both control systems are described in the following subsections.

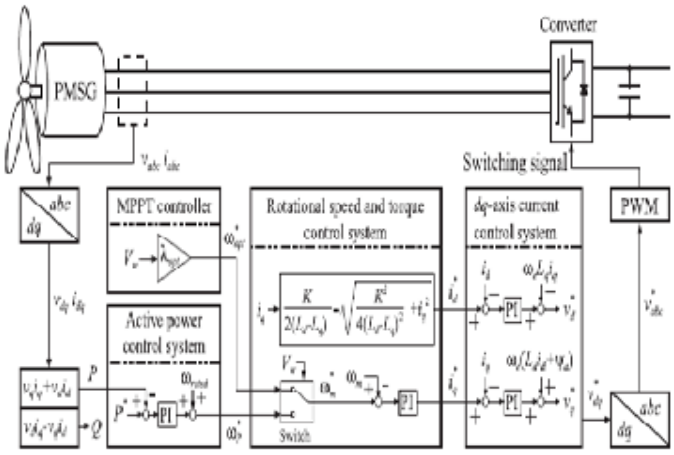

Fig.2.4. Configuration of proposed converter control system

2.4.1 Rotational speed and torque control

System

The rotational speed and torque control systems are shown in Fig. 2.4. The error between the reference rotational speed and measured rotational speed is processed through a PI controller. The controller generates the *q*-axis reference current I*d-q*. Output power characteristics of the WECS are depicted in Fig.2.4.5. Dots represent maximum power points for the discrete steps in wind speed. Each power curve contains the optimal rotational speed yopt corresponds to maximum wind power generation. In MPPT control area (Region 2), the pitch angle *b* is set to 2◦. Here, the optimal rotational speed yopt is represented by optimal tip speed ratio kopt and wind velocity Vw as follows:

$$\omega_{opt}=\lambda_{opt}V_W \quad (9)$$

If the rotational speed ym is equal to the optimal rotational speed yopt, the output power will be maximum. In this paper, a salient-pole type PMSG is used. In order to achieve the maximum torque from the PMSG, the d-axis reference current Id is determined by the above equation.

2.4.2. Active power control system

The active power control system is shown in Fig. 2.4.2 The reference rotational speed Yw is the sum of the rated rotational speed yrated and the output of the PI based power controller. This output is a correction value to compensate the performance of the power tracking reference. The controller is used for the rated power control (Region 3) and power suppression control (Region 4). In Region 3, the reference power Pw is equal to the rated power Prated. In Region 4, the output command value is decreased linearly according to the increase in the wind speed. A sudden disconnection from the power system is prevented and the operating region of the wind speed is considered up to 35 m/s.

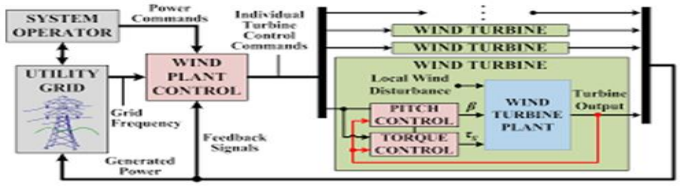

Fig.2.4.2. Active Power Control

2.4.3 dq-Axis current control system

The dq-axis current control system is shown in Fig. 2.4. This a decoupling based synchronous frame PI controller where the d-axis and q-axis current errors are processed though the respective PI controllers. Then decoupling terms are added or subtracted to produce d-axis and q-axis reference voltages V-dq.

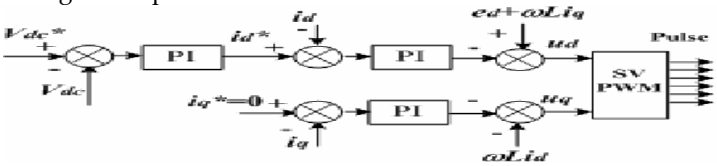

Fig.2.4.3. dq-Axis Current Control

2.4.4 Pitch angle control system

The pitch angle control is applied for Regions 3 and 4 as it needed for the output power control. The conventional pitch angle control system is shown in Fig.2.4.4 In this method, the output power of the PMSG is controlled by using only the pitch angle control system. The pitch angle command value bCMD is obtained from the PI controller. Input of the PI controller is the deviation between the power command value Pw and the measured output power P. The output power command value Pw is set as the rated power Prated (2MW) in Region 3. The operating mechanism of the pitch angle control is realized by a hydraulic servo system. The hydraulic servo system has 0.1 s time lag and the operating speed of the pitch angle control is ±10◦/s. The tracking speed and accuracy of the conventional pitch angle control are not so good as the pitch changing speed is slow. The proposed pitch angle controller will try to improve the performance.

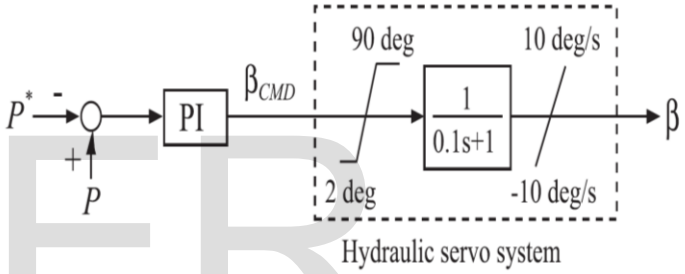

Fig.2.4.4 (a). Conventional Pitch Angle Control

The proposed pitch angle control system is shown in Fig.2.4.4(a). In this method, reference pitch is correlated with wind speed rather than the power. The pitch angle reference bw in the Regions 3 and 4 is determined by a lookup table as shown in Fig.2.4.4(b). The pitch angle reference is designed so that it makes the rotational speed lower than the rated rotational speed. When the wind speed is more than 25 m/s, the rotational speed is sufficiently reduced. However, excessive reduction in rotational speed requires small pitch angles and excessive mechanical torques. Hence, the balance of stresses due to centrifugal force and mechanical torque are regulated by the proposed pitch angle reference.

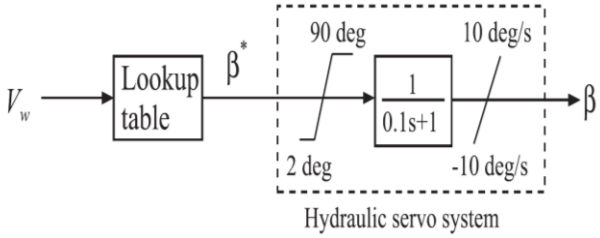

Fig.2.4.4 (b).Proposed Pitch Angle Control

2.4.5 Control strategy of power generation

shows a typical WECS output power curve for the

conventional and proposed controls with respect to the pitch angle. First the conventional control strategy is described. The dotted line on Fig.2.4.5. indicates the conventional control strategy. When the wind velocity is between 5 and 12 m/s, MPPT control is utilized for the WECS to generate maximum power. The MPPT control is performed by controlling the rotational speed due to adjusting the duty ratio of the MSC as well as the generator currents. The pitch angle control is activated so that the output power remains constant at the rated power when the wind velocity is between 12 and 25 m/s. If the wind velocity reaches 25 m/s, the wind generator is turned-off, and the pitch angle is set as 90◦. In general, if the averaged wind velocity over 10 min is more than 25 m/s or the averaged wind velocity averaged over 3 s is more than 30 m/s, the wind generation is forced to switch-off. Next, the proposed control strategy is described.

Indicates the proposed control strategy for power generation as a solid line. Moreover, the wind speed ranges are shown as Regions 1, 2, 3, and 4. In Region 2, the proposed control method is same as the conventional method. In Region 3, not only the pitch angle control but also rotational speed control are adopted for the WECS. The hybrid control enables high-precision output control. The proposed method can ensure safety in strong wind conditions because it decreases the rotation speed as the wind speed increases.

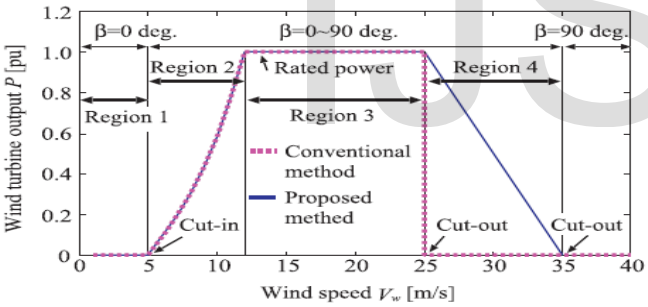

Fig.2.4.5. Output Control Strategy

The main stresses on the wind turbine are aerodynamic loads on the blade and centrifugal force. Particularly, the centrifugal force is a product of rotational velocity squared and mass, which always acts radial outward, hence the raised load demands of higher tip speeds. Therefore, the proposed method preferentially reduces the rotational speed rather than the mechanical torque during the strong wind condition. As a result, the allowable condition of power generation can temporarily reach up to the wind speed from 25 m/s to 35 m/s in Region 4 because the proposed control significantly reduces the power coefficient and the centrifugal force. In other words, the power generation is continued until the averaged wind velocity over 10 min exceeds 30 m/s or the averaged wind velocity over 3 s exceeds 35 m/s which helps to improve the overall efficiency of the PMSG based WECS.

3 Simulation And Results

In this section, the conventional and proposed methods are compared based on same conditions. Note that the same conditions mean that the wind velocity, PMSG parameters, wind turbine parameters and parameters of PI controller are same in both models. These parameters of PI controller are chosen by empirical knowledge. Table 1 shows the parameters of the wind turbine and PMSG. In Operation of wind turbine under a linear wind velocity, conventional and proposed methods are compared under a linear wind velocity with small oscillations as shown in Fig. 9a and the simulation results are shown for all the operating regions. In Operation of wind turbine under a wind velocity when a typhoon is landed, these two methods are compared under a wind velocity when the typhoon is landed as shown in Fig. 9b. Therefore, the realistic behaviour of wind turbines is demonstrated.

3.1 Simulation Parameters

Parameters of wind turbine	
Blade radius *R*	38m
Air density *q*	1.205 kg/m3
Rated wind speed *Vw rated*	12 m/s
Optimal tip speed ratio *kopt*	0.187
Parameters of PMSG	
Rated output *Prated*	2MW
Resistance *Ra*	50 *lY*
d axis inductance *Ld*	5.5mH
q axis inductance *Lq*	3.75mH
Number of pole pairs *p*	11
Field flux *K*	136.25V• s/rad
Inertia *J*	10,000 kg •m2

Table 3.1. Simulation Parameters

3.2 Operation of Wind Turbine Under A Linear Wind Velocity

The wind speed increases from 8 to 35 m/s as shown in Fig.3.2(a). Therefore, it satisfies all the operating regions of WECSs. In Region 2, both models perform the MPPT control. In Region 3, the output power with the conventional system follows the reference with oscillations because it is controlled by only pitch angle control. However, the output power with the proposed control exactly follows its reference. This is due to the employment of not only pitch angle control but also rotational speed control. In Region 4, the generated power with the conventional system is suddenly dropped when wind velocity exceeds 25 m/s. On the other hand, the generated

power with the proposed system is suppressed to less than the rated power and generation is continued In Region 2, both mechanical rotational speeds are same because the same MPPT control is applied. In Region 3, the mechanical rotational speed with the conventional method is constant. Conversely, the proposed method controls the rotational speed to accurately adjust the generated power. Furthermore, it can ensure safety because the rotation speed is decreased in strong wind conditions to suppress

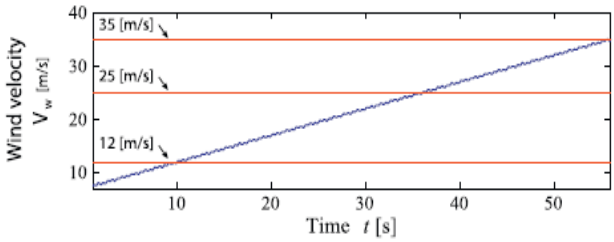

Fig.3.2 (a). Linear wind velocity with small oscillations

3.2.1. Results for Small wind Conditions

4. Conclusion

This paper describes a control method for the PMSG based WECS under strong wind conditions. Conventional control methods compared with the proposed control method considering same conditions and system parameters. In the MPPT control area, both conventional and proposed systems have shown similar performances. When the wind turbine is controlled at the rated power, the power fluctuation occurs with the conventional method. This is because; it is controlled by only the pitch angle control system with some delays. In the proposed method, both pitch angle and rotational speed control methods are designed for the wide-wind range of wind velocity. As a result, the output power is controlled with high accuracy by using the proposed method. In addition, the proposed method preferentially reduces the rotational speed rather than the mechanical torque in order to reduce the power coefficient and the centrifugal force during the strong wind conditions. For this reason, the allowable condition of power generation can temporarily reach up to the wind speed of 35 m/s. Therefore, it can be said that the PMSG based WECS with the proposed control method can avoid a sudden cut-off from the power grid during strong wind conditions as well as can continue to generate power in the typhoon prone area. However, if the wind speed goes above the 35 m/s the time to bring appropriate load-frequency control action rather than sudden generation curtailment.

Acknowledgment

Dr.D.Chandra Sekhar received B.Tech Degree in Electrical and Electronics Engineering, M.Tech Degree in Power System Operation and Control in Electrical and Electronics Engineering, Ph.D Degree from Sri Venkateswara University College of Engineering (Sri Venkateswara University) Tirupati, Andhra Pradesh, India in 2005, 2009 and 2019 respectively. .Currently working as a Professor and Head of the Department in Electrical and Electronics Enginering,VEMU Institute Of Technology,P.Kothakota ,Chittoor, Andhra Pradesh,India.

MISS V.GEETHA RECEIVED B.TECH DEGREE FROM MADHIRA COLLEGE OF ENGINEERING, KODAD, CHITTOOR DIST, TELANGANA STATE, INDIA AND RECEIVED M.TECH DEGREE IN ELECTRICAL POWER SYSTEMS IN K.V.SUBBAREDDY WOMENS ENGINEERING COLLEGE, KURNOOL DIST, A.P, INDIA. CURRENTLY WORKING AS AN ASSISTANT PROFESSOR IN DEPARTMENT OF EEE IN VEMU INSTITUTE OF TECHNOLOGY P.KOTHAKOTA, CHITTOOR DIST, A.P, INDIA.

REFERENCES

[1] Aho, J., Buckspan, A., Laks, J., Fleming, P., Jeong, Y., Dunne, F., ... Johnson, K. (2012). A tutorial of wind turbine control for supporting grid frequency through active power control. *2012 American Control Conference (ACC)*. (pp. 3120–3131). https:// doi.org/10.1109/ACC.2012.6315180.

[2] Ajami, A., Alizadeh, R., & Elmi, M. (2016). Design and control of a grid tied 6-switch converter for two independent low power wind energy resources based on pmsgs with mppt capability. *Renewable Energy*, *87*(Part 1), 532–543. https://doi.org/10. 1016/j.renene.2015.10.031.

[3] Bonfiglio, A., Delfino, F., Invernizzi, M., & Procopio, R. (2017). Modeling and maximum power point tracking control of wind generating units equipped with permanent magnet synchronous generators in presence of losses. *Energies*, *10*(1), https://doi. org/10.3390/en10010102.

[4] Cader, C., Bertheau, P., Blechinger, P., Huyskens, H., & Breyer, C. (2016). Global cost advantages of autonomous solar-battery-diesel systems compared to diesel-only systems. *Ener-*

gy for Sustainable Development, *31*(Supplement C), 14–23. https:// doi.org/10.1016/j.esd.2015.12.007.

[5] Chen, J., & Song, Y. (2016). Dynamic loads of variable-speed wind energy conversion
system. *IEEE Transactions on Industrial Electronics*, *63*(1), 178–188. https://doi.org/ 10.1109/TIE.2015.2464181.

[6] Cooney, C., Byrne, R., Lyons, W., & O'Rourke, F. (2017). Performance characterisation of a commercial-scale wind turbine operating in an urban environment, using real data. *Energy for Sustainable Development*, *36*(Supplement C), 44–54. https://doi. org/10.1016/j.esd.2016.11.001.

[7] Dahbi, A., Nait-Said, N., & Nait-Said, M.-S. (2016). A novel combined mppt-pitch angle control for wide range variable speed wind turbine based on neural network. *International Journal of HydrogenEnergy*,*41*(22),9427–9442
http://www.sciencedirect.com/science/article/pii/S0360319916303172.https://doi.org/10.1016/j.ijhydene.2016.03.105.

[8] Domenech, B., Ferrer-Martí, L., Lillo, P., Pastor, R., & Chiroque, J. (2014). A community electrification project: Combination of microgrids and household systems fed by wind, pv or micro-hydro energies according to micro-scale resource evaluation and social constraints. *Energy for Sustainable Development*, *23*(Supplement C), 275–285. https://doi.org/10.1016/j.esd.2014.09.007.

[9] dos Santos, L., Canha, L., & Bernardon, D. (2018). Projection of the diffusion of photovoltaic
systems in residential low voltage consumers. *Renewable Energy*, *116*(Part
A), 384–401. https://doi.org/10.1016/j.renene.2017.09.088.

[10] Giallanza, A., Porretto, M., Cannizzaro, L., & Marannano, G. (2017). Analysis of the maximization of wind turbine energy yield using a continuously variable transmission system. *Renewable Energy 102*,(Part B), 481–486. https://doi.org/10.1016/j.renene.2016.10.067.

[11] Huang, C., Li, F., & Jin, Z. (2015). Maximum power point tracking strategy for large-scale wind generation systems considering wind turbine dynamics. *IEEE Transactions on Industrial Electronics*, *62*(4), 2530–2539. https://doi.org/10.1109/TIE.2015.2395384.

[12] Kobayakawa, T., & Kandpal, T. C. (2016). Optimal resource integration in a decentralized renewable energy system: Assessment of the existing system and simulation for its expansion. *Energy for Sustainable Development*, *34*(Supplement C), 20–29. https://doi.org/10.1016/j.esd.2016.06.006.

[13] Oliver, T., Lew, D., Redlinger, R., & Prijyanonda, C. (2001). Global energy efficiency and renewable energy policy options and initiatives. *Energy for Sustainable Development*, *5*(2), 15–25. https://doi.org/10.1016/S0973-0826(08)60266-5.

[14] Rodríguez-Amenedo, J., Arnaltes, S., & Rodríguez, M. (2008). Operation and coordinated
control of fixed and variable speed wind farms. *Renewable Energy*, *33*(3), 406–414. https://doi.org/10.1016/j.renene.2007.03.003.

[15]Shamsul, N., Kamarudin, S., & Rahman, N. (2017). Conversion of bio-oil to bio gasoline via pyrolysis and hydrothermal: A review. *Renewable and Sustainable Energy Reviews*, *80*(Supplement C), 538–549. https://doi.org/10.1016/j.rser.2017.05.245.

[16] Shokrieh, M. M., & Rafiee, R. (2006). Simulation of fatigue failure in a full composite wind turbine blade. *Composite Structures*, *74*(3), 332–342. https://doi.org/10.
1016/j.compstruct.2005.04.027.

[17] Tiwari, R., Padmanaban, S., & Neelakandan, R.B. (2017). Coordinated control strategies for a permanent magnet synchronous generator based wind energy conversion system. *Energies*, *10*(10), https://doi.org/10.3390/en10101493.

[18] Uehara, A., Pratap, A., Goya, T., Senjyu, T., Yona, A., Urasaki, N., & Funabashi, T. (2011). A
coordinated control method to smooth wind power fluctuations of a PMSG-based WECS. *IEEE Transactions on Energy Conversion*, *26*(2), 550–558. https://doi.org/10.1109/TEC.2011.2107912.

[19] Wei, C., Zhang, Z., Qiao, W., & Qu, L. (2015). Reinforcement-learning-based intelligent maximum power point tracking control for wind energy conversion systems. *IEEE Transactions on Industrial Electronics*, *62*(10), 6360–6370. https://doi.org/10.1109/ TIE.2015.2420792.

[20] Wei, C., Zhang, Z., Qiao, W., & Qu, L. (2016). An adaptive network-based reinforcement learning method for mppt control of pmsg wind energy conversion systems. *IEEE Transactions on Power Electronics*, *31*(11), 7837–7848. https://doi.org/10.1109/ TPEL.2016.2514370.

[21] Yao, J., Liu, R., Zhou, T., Hu, W., & Chen, Z. (2017). Coordinated control strategy for hybrid wind farms with dfig-based and pmsg-based wind farms during network unbalance. *Renewable Energy*, *105*(Supplement C), 748–763. https://doi.org/10. 1016/j.renene.2016.12.097.

[22] Yin, M., Li, G., Zhou, M., & Zhao, C. (2007). Modeling of the wind turbine with a permanent magnet synchronous generator for integration. *2007 IEEE Power Engineering Society General Meeting*. (pp. 1–6). https://doi.org/10.1109/PES.2007.385982.

[23] Yoon, J., He, D., & Hecke, B. V. (2015). On the use of a single piezoelectric strain sensor for wind turbine planetary gearbox fault diagnosis. *IEEE Transactions on Industrial Electronics*, *62*(10), 6585–6593. https://doi.org/10.1109/TIE.2015.2442216.

[24] Yuan, Y., & Tang, J. (2017). Adaptive pitch control of wind turbine for load mitigation
under structural uncertainties. *Renewable Energy*, *105*, 483–494. https://doi.org/ 10.1016/j.renene.2016.12.068.